Supplement of The Cryosphere, 15, 2041–2055, 2021
https://doi.org/10.5194/tc-15-2041-2021-supplement

The Cryosphere Open Access EGU

Supplement of

Top-of-permafrost ground ice indicated by remotely sensed late-season subsidence

Simon Zwieback and Franz J. Meyer

Correspondence to: Simon Zwieback (szwieback@alaska.edu)

Table S1: Cores from 2005.

Name	Lat/lon [°]	Ice rich	Site and core description
05-1	67.786/-164.474	1	perimeter of low-centred polygon in uplands massive ice
05-2	67.786/-164.474	1	interior of low-centred polygon in uplands silt with up to 40% visible ice
05-3	67.811/-164.563	1	tussock-covered hillslope silt with 40% visible ice
05-4	67.816/-164.598	1	non-sorted circle in polygon interior; gentle hillslope massive ice
05-5	67.821/-164.592	1	tussock-covered interior of; gentle hillslope massive ice and ice-rich silt (30% visible ice)
05-6	67.823/-164.609	1	interior of low-centred polygon on edge of drainage ice inclusions in peat and massive ice
05-7	67.845/-164.735	0	gravel-covered bench gravel with 5% visible ice
05-8	67.849/-164.726	1	tussock-covered interior of faint polygon colluvial silt with 30 to 40% visible ice
05-9	67.847/-164.731	1	tussock-covered colluvium silt and gravel: 50% visible ice
05-10	67.843/-164.740	1	tussock-covered interior of faint polygon colluvial silt 30% visible ice (lenses up to 5 mm thick)
05-11	67.845/-164.725	1	tussock-covered hillslope; colluvium ice with soil inclusions: 50 to 60% visible ice
05-12	67.847/-164.721	1	tussock-covered hillslope; colluvium sandy, gravelly silt with 40 to 50% visible ice
05-13	67.851/-164.732	1	tussock-covered hillslope; colluvium sandy silt with ice lenses up to 5 mm thick
05-14	67.849/-164.737	1	tussock-covered hillslope; colluvium silt with 15–20% visible ice; ice with silt inclusions

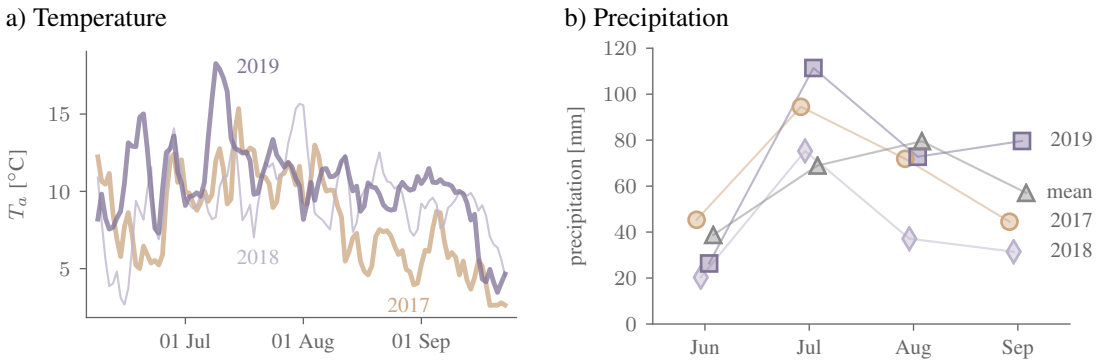

Figure S1: Meteorological time series for Kivalina from the MERRA-2 reanalysis: a) air temperature T_a; b) monthly precipitation for 2017–2019 and the 30-year average. Large precipitation amounts exceeding 100 mm in July 2019 are confirmed by in-situ observations, whose coverage during the rest of the study period is poor.

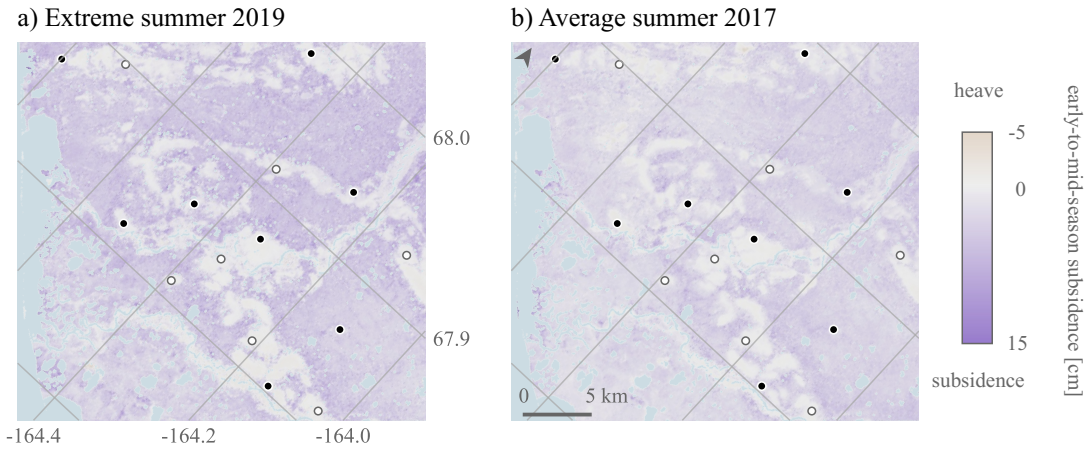

Figure S2: Early–mid-season subsidence (10 June – 10 August) for 2017 and 2019; otherwise identical to Fig. 5a–b)

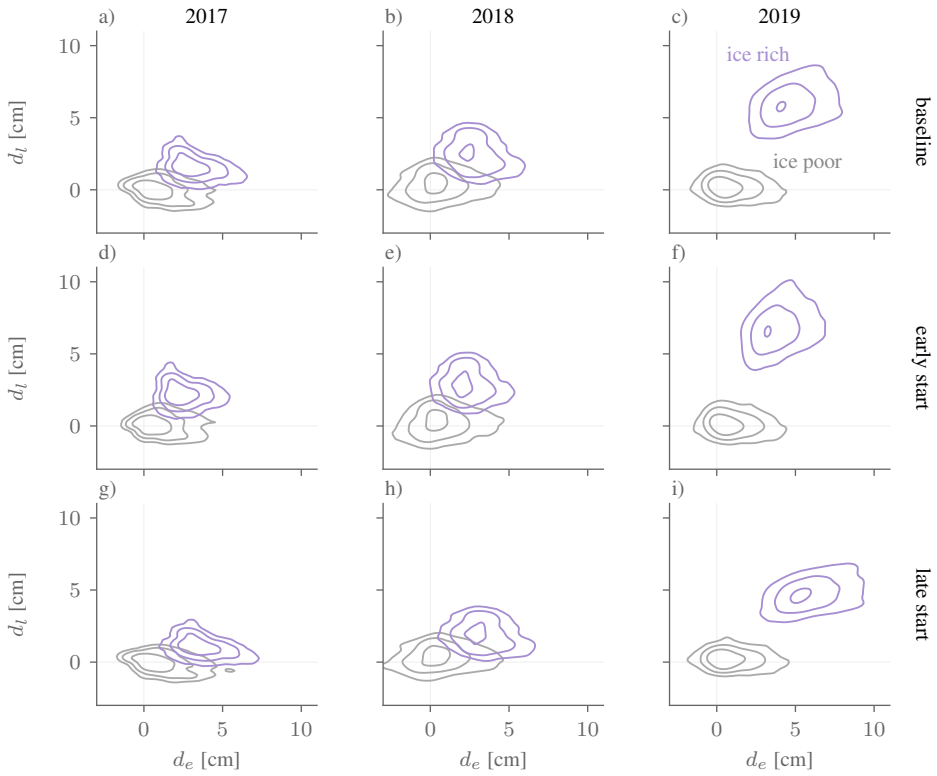

Figure S3: Contour plots of a kernel density estimate of the early–mid-season and late-season subsidence for ice rich (purple) and ice poor (grey), as determined independently by manual mapping. The columns correspond to the year; the rows to the beginning of the late season: baseline: 10 August, early start: 31 July, late start: 20 August.